

## V. NUCLEAR MAGNETIC RESONANCE AND HYPERFINE STRUCTURE

Prof. F. Bitter	R. L. Fork	P. G. Mennitt
Prof. J. S. Waugh	J. V. Gaven, Jr.	S. R. Miller
Dr. L. C. Bradley III	Ilana Levitan	O. Redi
Dr. H. H. Stroke	F. A. Liégeois	C. J. Schuler, Jr.
Dr. J. F. Waymouth	F. Mannis	W. W. Smith
T. Fohl	I. G. McWilliams	W. T. Walter

### A. NUCLEAR RELAXATION IN VARIOUS FERROELECTRIC CRYSTALS

From various studies of crystal structure, and particularly from measurements of the deuterium isotope effect on the Curie temperature  $T_c$ , it is clear that the hydrogen atoms play an important role in the ferroelectric or antiferroelectric properties of many crystals, including the well-known examples of Rochelle salt and  $\text{KH}_2\text{PO}_4$ .<sup>1</sup> Proton resonance linewidth studies have previously been made on some of these substances, but, in general, with disappointing results.<sup>2</sup> The idea is that if the H atoms are involved in the transition, some appreciable change in their positions or rates of motion ought to occur there. Unfortunately, the structure changes expected are not usually such as to lead to large changes in linewidth, and no change in the rate of motion will be observed unless the latter crosses the critical region for linewidth changes ( $10^4$ - $10^5 \text{ sec}^{-1}$ ) near  $T_c$ .

When, as is often true, the proton spin-lattice relaxation time  $T_1$  is governed by the motions of the protons that are of interest, longitudinal relaxation measurements offer a much sharper tool for investigating the internal motions in these crystals. We have just finished a series of such measurements on a number of inorganic salts exhibiting ferroelectric or antiferroelectric behavior with results that can be briefly summarized as follows:

$(\text{NH}_4)_2\text{SO}_4$ :  $T_1$  drops abruptly on entering the ferroelectric phase and the barrier to  $\text{NH}_4^+$  reorientation increases from  $2.3 \pm 1.1$  to  $6.1 \pm 1.2$  kcal/mole.

$(\text{NH}_4)_2\text{BeF}_4$ : The slope, but not the magnitude, of the  $T_1$  vs  $\frac{1}{T}$  plot changes at the Curie point. The  $\text{NH}_4^+$  barrier is  $5.3 \pm 1.2$  kcal/mole in the ferroelectric phase, and  $1.5 \pm 0.7$  kcal/mole in the paraelectric phase.

$(\text{NH}_4)_2\text{SO}_4 - (\text{NH}_4)_2\text{BeF}_4$  Solid Solutions: In general, intermediate behavior between the two pure salts is observed except that the  $\text{NH}_4^+$  barriers are somewhat higher, approximately 10 kcal/mole, in the ferroelectric phases. The measurements are summarized in Fig. V-1.

$\text{NH}_4\text{HSO}_4$ : At the upper Curie point ( $-30^\circ\text{C}$ ) only a small change in the activation energy occurs. At the lower Curie point ( $-119^\circ\text{C}$ ) there is an abrupt change in  $T_1$  accompanied by a sharp rise in the  $\text{NH}_4^+$  barrier in the low temperature phase (cf. Fig. V-2). These results suggest that the upper transition is primarily connected with a rearrangement of protons in O-H-O hydrogen bonds and that the lower transition is, as in the salts mentioned above, connected with an ordering of the ammonium ions.

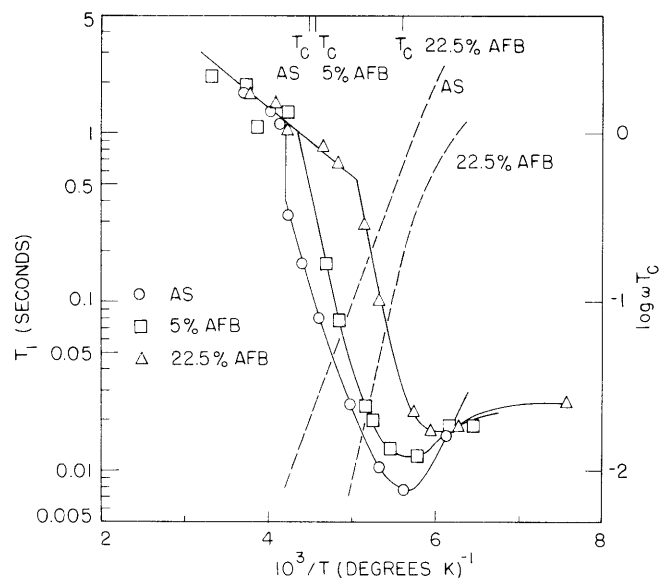


Fig. V-1. Proton  $T_1$  (solid curves), and correlation times at  $\omega = 2\pi \times 30$  mc (dashed curves) for  $(\text{NH}_4)_2\text{SO}_4$  (AS) and its solid solutions with  $(\text{NH}_4)_2\text{BeF}_4$  (AFB).

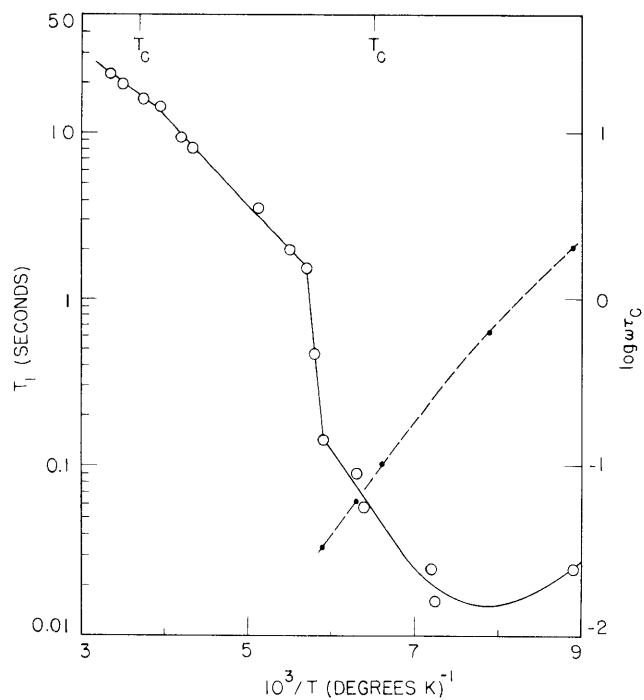


Fig. V-2.  $T_1$  and correlation time vs temperature for the protons in  $\text{NH}_4\text{HSO}_4$ .

## (V. NUCLEAR MAGNETIC RESONANCE)

$(\text{NH}_4)_2\text{H}_3\text{IO}_6$ : The thermal relaxation is nonexponential at all temperatures, but can be decomposed into two exponentials with relative weights about 5:2 each of which, by itself, leads to exactly the same dependence of correlation time  $\tau_c$  on temperature. The activation energy of approximately 2 kcal/mole can be clearly associated with the reorientation of  $\text{NH}_4^+$  ions. No change in either  $T_1$  or its slope occurs at  $T_c$ ; this suggests that the "acid" hydrogen atoms are primarily responsible for the ferroelectricity, as, apparently, they are in  $\text{Ag}_2\text{H}_3\text{IO}_6$ . The nonexponential relaxation may be connected with the effects of correlation, as first suggested by Hubbard.<sup>3</sup>

$\text{Ag}_2\text{H}_3\text{IO}_6$ :  $T_1$  is greater than 1 sec and independent of temperature, except for a small dip near  $T_c$ . Probably paramagnetic impurities are involved.

$\text{CaB}_3\text{O}_4(\text{OH})_3 \cdot \text{H}_2\text{O}$  (Colemanite): No change in  $T_1$  or its slope occurs at  $T_c$  ( $-2.5^\circ\text{C}$ ), and a single thermally activated motion with a barrier of  $4.9 \pm 1.1$  kcal/mole is found, this being apparently the same motion that is responsible for a linewidth transition at approximately  $-60^\circ\text{C}$ . It is probable that the relaxation of both OH and  $\text{H}_2\text{O}$  protons occurs through motions of water molecules. Further interpretation is difficult.

$\text{K}_4\text{Fe}(\text{CN})_6 \cdot 3\text{H}_2\text{O}$ : Only linewidth and infrared measurements were made on this salt. A gradual linewidth transition occurs near  $200^\circ\text{K}$  and can be interpreted in terms of a barrier of 2.5 kcal/mole to the reorientation of a water molecule. From the magnitude of the second moment at low temperatures, it has been possible to suggest a tentative set of hydrogen atom positions.

Detailed accounts of all of these measurements and their interpretation are in the process of publication. This work was carried out in collaboration with Dr. R. Blinc, who is now at the School for Advanced Study, M.I. T., on leave from the Stefan Institute, Ljubljana, and Dr. M. Brenman, who is here on leave from the National Microbiological Institute, Buenos Aires, Argentina.

J. S. Waugh, S. R. Miller

### References

1. H. D. Megaw, *Ferroelectricity in Crystals* (Methuen and Company, Ltd., London, 1957).
2. G. Burns, *Phys. Rev.* 123, 64 (1961).
3. P. S. Hubbard, *Phys. Rev.* 109, 1153 (1958).

## B. PARITY CONSERVATION IN MOLECULES

We have succeeded in making a measurement of high accuracy in the experiment outlined in Quarterly Progress Report No. 60 (page 91), in which we search for evidence of parity nonconservation in molecular oxygen. In this experiment, we attempt to

## (V. NUCLEAR MAGNETIC RESONANCE)

observe circular dichroism (preferential absorption of one circular polarization) in the forbidden magnetic dipole transition  $^3\Sigma_g^- \rightarrow ^1\Sigma_g^+$  of  $O_2^{16}$ . The oxygen, at atmospheric pressure, is placed in an absorption cell of 2.4 meters length. The light source is an electrodeless discharge in krypton gas, placed in a magnetic field; it happens that a strong line of krypton ( $\lambda 7601 \text{ \AA}$ ) nearly coincides with one line of the O-O oxygen band, and a magnetic field of  $\pm 4000$  gauss is sufficient to shift the  $\sigma_{\pm}$  components of the krypton line to give maximum absorption. The absorption is measured by observing the light emitted parallel to the magnetic field; the light is passed through a quarter-wave plate followed by a polaroid rotating at 15 cps. A 30-cps signal in a photomultiplier placed behind the absorption cell then shows that the  $\sigma_{+}$  radiation is being absorbed more than the  $\sigma_{-}$  (or vice versa, depending on the phase), and therefore measures the absorption.

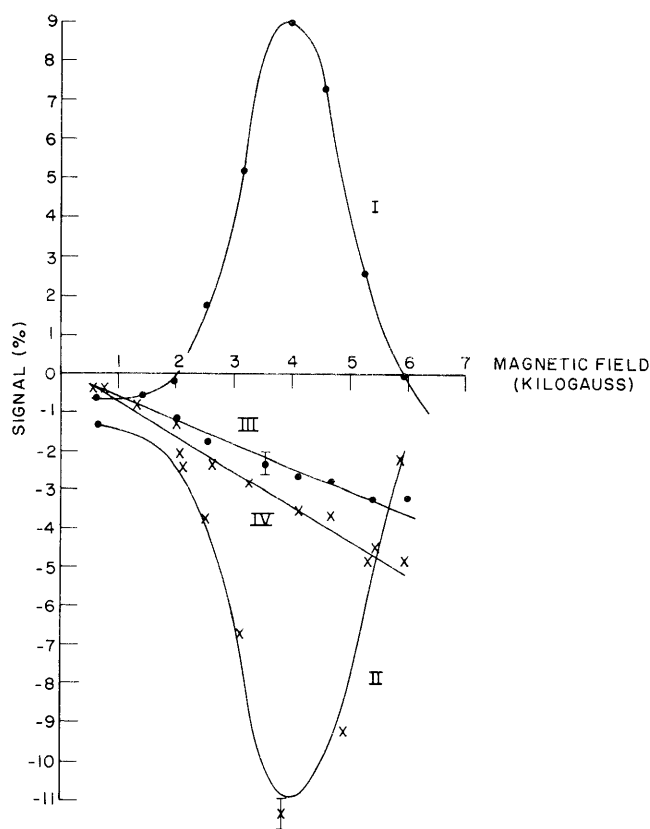


Fig. V-3. Curves I and II: Absorption signal as a function of magnetic field, for positive and negative fields, respectively. Curves III and IV: Circular polarization signal ( $\times 10$ ) as a function of magnetic field, for positive and negative fields, respectively.

Curves I and II in Fig. V-3 show the absorption peak for positive and negative fields, respectively; the change in sign shows the change of phase expected when the field is

reversed. The observed absorption has a width resulting, principally, from pressure broadening; it has been fitted to a Lorentzian shape with width  $0.114 \text{ cm}^{-1}$ , and cross-section at maximum,  $\sigma_0 = 5.2 \times 10^{-22} \text{ cm}^2$ . This leads to a value for the oscillator strength  $f = 1.02 \times 10^{-10}$ , which is smaller by a factor of  $\sim 10$  than the measurements of Childs and Mecke.<sup>1</sup> The observed linewidth may be compared with the expected Doppler width of  $0.029 \text{ cm}^{-1}$ .

The measurement of circular dichroism is accomplished by replacing the rotating polaroid with a fixed polaroid so that only the components absorbed by the oxygen are transmitted, and following this with a quarter-wave plate rotating at 15 cps. A 30-cps signal is then interpreted as the circular dichroism to be measured. Curves III and IV show the observations for positive and negative fields, respectively (multiplied by ten). The fact that there is no maximum (within experimental error) at the fields corresponding to the absorption maxima shows that the observed signal is an artifact, which we believe to be due to the fact that the discharge moves about in its cylindrical container as the field is varied, and the polarization of the emitted light therefore changes on account of the oblique incidence on the cylindrical walls.

We conclude that our observed circular dichroism (defined as  $\frac{\sigma_+ - \sigma_-}{\sigma_+ + \sigma_-}$ , where  $\sigma_{\pm}$  are the absorption cross sections for the two circular polarizations) is less than  $6 \times 10^{-4}$  in absolute value. Blin-Stoyle<sup>2</sup> has shown that this quantity is given to a good approximation by  $\frac{2a|E|}{|M|}$ , where  $a$  is the amplitude of the mixing coefficient for an odd-parity state (say  ${}^3\Sigma_u^-$ ) into either the upper or lower state, and  $|E|$  and  $|M|$  are the reduced matrix elements for electric and magnetic dipole transitions,  ${}^3\Sigma_u^- - {}^3\Sigma_g^-$  and  ${}^1\Sigma_g^+ - {}^3\Sigma_g^-$ , respectively. Now  $\frac{|E|}{|M|} = \left(\frac{f_E}{f_M}\right)^{1/2}$ , and with  $f_E \sim 0.1$ , typically, and  $f_M = 10^{-10}$ , we find  $|a| \leq 10^{-8}$ . Thus within the accuracy of our measurements parity is conserved in the oxygen molecule.

We are proceeding with our experiment in the hope of further refining it and of extending it to the transition  ${}^3\Sigma_g^- \rightarrow {}^1\Delta_g$  of  $\text{O}_2$ . Meanwhile, an attempt is being made to interpret our result in terms of a number of theoretical possibilities.

L. C. Bradley III, N. S. Wall

(Professor Wall is from the Laboratory for Nuclear Science, M.I.T.)

#### References

1. W. H. J. Childs and R. Mecke, Z. Physik 68, 344 (1931).
2. R. J. Blin-Stoyle, Phys. Rev. 120, 181 (1960).

## (V. NUCLEAR MAGNETIC RESONANCE)

### C. MERCURY 197-199 HYPERFINE-STRUCTURE ANOMALY

Nuclear magnetic resonance between the ground state Zeeman sublevels  $m = \pm 1/2$  of the 65-hour radioisotope  $\text{Hg}^{197}$  was reported in Quarterly Progress Report No. 62 (page 105). The width of this resonance has now been reduced from 500 cps to 30 cps by improving the homogeneity of the Helmholtz field at the position of the cell containing  $\text{Hg}^{197}$  vapor. Figure V-4 shows a pair of resonances at 360 kc in a field of 450 gauss. The old set of Helmholtz coils has been replaced by a set of L-128 coils from Harvey-Wells Corporation. Each coil consists of 800 turns of a 5 1/4 in.  $\times$  0.008 in. copper tape and has a resistance of 0.8 ohm. The mean diameter of these coils is 19 5/16 inches, which is a little more than twice the 8 3/4-inch diameter of the old coils. The L-128 coils have been connected in series, and approximately 18 ohms of resistance has been connected across the stronger of the two coils to produce equal fields at the centers of the two coils. A Harvey-Wells Magnet Power Supply (Model HS 1050) is used to stabilize the current through the coils to 1 part in  $10^5$ , and a proton resonance probe placed 1 inch from the cell is used to monitor the field before and after each mercury resonance.

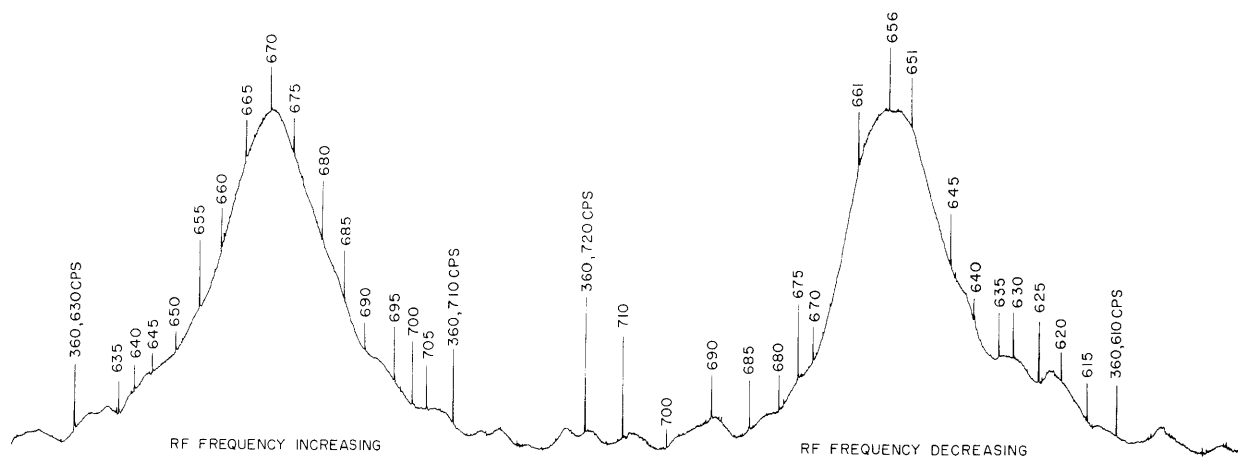


Fig. V-4.  $\text{Hg}^{197}$  ground sublevel resonances. (Proton resonant frequency was 1,940,545 cps throughout both resonances.)

A cell has been successfully filled with sufficient amounts of both  $\text{Hg}^{197}$  and  $\text{Hg}^{199}$  to observe nuclear magnetic resonance of each isotope. The correct frequency of circularly polarized optical pumping light for each isotope was obtained by changing the magnetic field about an  $\text{Hg}^{202}$  lamp. If this change in the scanning field does not influence the Helmholtz splitting field about the cell, each set of atoms will see the same magnetic field; and a direct measurement of the ratio of the magnetic moments,  $\mu_{197}/\mu_{199}$  can be made. The first results from the use of this technique,  $\mu_{197}/\mu_{199} = 1.0425 (\pm 1)$ ,

## (V. NUCLEAR MAGNETIC RESONANCE)

are an improvement over the earlier value.<sup>1</sup> Comparison with the ratio of Stager's values<sup>2</sup> of the interaction constants for the  $^3P_1$  state,  $A_{197}/A_{199} = 1.043284 (\pm 1)$ , indicates a hyperfine-structure anomaly of  $0.75 \pm 0.1$  parts in 1000.

Work is continuing to shield the scanning field from the splitting field and to improve the precision of the value of this anomaly.

W. T. Walter

### References

1. W. T. Walter, Quarterly Progress Report No. 62, Research Laboratory of Electronics, M.I.T., July 15, 1961, p. 105.
2. C. V. Stager, Hyperfine Structure of  $Hg^{197}$  and  $Hg^{199}$ , Ph.D. Thesis, Department of Physics, M.I.T., 1960.

### D. A COMPACT MAGNETO-OPTIC SCANNING APPARATUS

In studies of the hyperfine structure of mercury which have been carried out before in this laboratory, lamps containing a single isotope (usually  $Hg^{198}$ ) functioned as a variable-frequency light source when placed in a magnetic field of up to 10,000 gauss.<sup>1</sup> The magnets used for this Zeeman-scanning work have heretofore been large air-core Bitter solenoids with inside diameters up to 4.5 inches, and maximum fields of 50 kgauss, or more. Professor Bitter has suggested that a smaller magnet with a maximum field of approximately 10,000 gauss might be more efficient, more portable, and easier to use for experiments with mercury (as well as for a number of other elements).

A suitable magnet has been designed and built by Magnion, Inc. (Model UFS-1) to our specifications. It is approximately a cube, roughly 7 inches on a side, and weighs approximately 100 lbs. It consists of a single, tape-wound, epoxy-covered coil (790 turns, resistance  $\approx 1$  ohm) surrounded by an iron core with two cylindrical pole caps (diameter,  $1 \frac{7}{8}$  inches), and has a 1-inch gap. A 0.25-inch axial hole has been drilled through the pole caps to let light out and 1-inch and 0.375-inch access holes run through the center of the coil, perpendicular to its axis. Low-pressure water cooling at a flow rate of 2-3 gal/min is sufficient to dissipate the heat produced in the coil at a power level of 3 kw (approximately 50 amps). At 50 amps, the magnet produces a field of 11.5 kgauss in the center of the gap. To achieve such a field in a 4-inch air-core Bitter solenoid requires approximately 100 kw power.

Current for the magnet is obtained from a power supply built by Henry R. Hirsch, consisting of a 230-volt, 3-phase motor-driven Variac and a full-wave solid-state rectifier bank with air-cooled heat sinks. The inductance of the magnet (calculated to be roughly 130 mh) is sufficient so that rms current ripple without additional filtering is estimated to be only 0.02 per cent at 4600 gauss, that is, approximately 1 gauss. This is, of course, negligible compared with the Doppler width of the

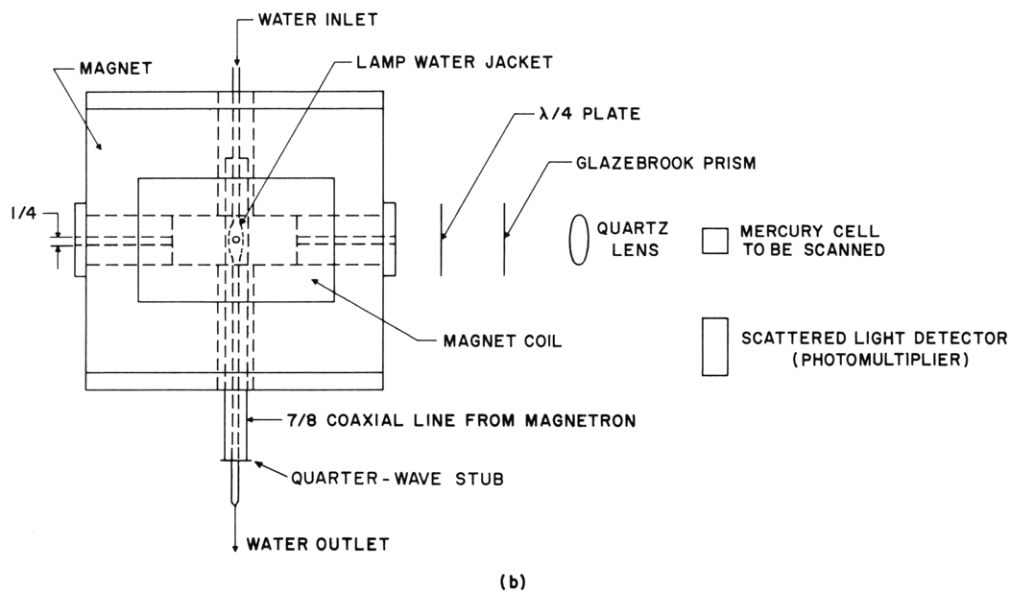
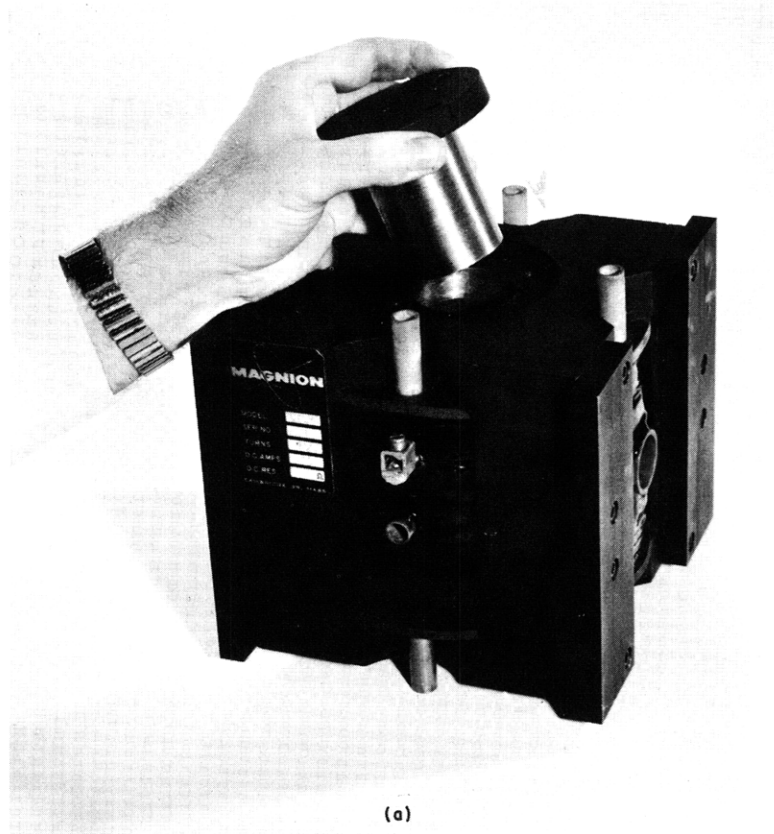


Fig. V-5. (a) The magnet. (b) Illustrating the use of the magnet in the scanning apparatus.



lamp in gauss, and hence should produce no modulation of the scattered light in a magnetic-scanning experiment.

The lamp used inside the magnet is similar to the one designed by Hirsch. It is water-cooled and is excited by microwaves.<sup>2</sup> The water inlet and outlet are concentric with the 0.25-inch diameter discharge tube inside the water jacket, and run through the center conductor of the 0.875-inch microwave coaxial line. The water tubes come out of the coaxial line through a right-angle bend by means of a hole drilled through the quarter-wave stub. The lamp must be run slightly warm to keep it from going out when the magnetic field is turned on. The intensity of the discharge is adequate for magnetic scanning and related experiments, in spite of the fact that the axial hole in the magnet is so small.

I would like to thank Dr. Henry R. Hirsch for his collaboration in the design of this apparatus.

W. W. Smith

#### References

1. See, for example, F. Bitter, S. P. Davis, B. Richter, and J. E. R. Young, *Phys. Rev.* 96, 1531 (1954); H. R. Hirsch, Photomultiplier bridge for magnetic-scanning experiments, Quarterly Progress Report No. 57, Research Laboratory of Electronics, M.I.T., April 15, 1960, pp. 60-61.

2. H. R. Hirsch, Water-cooled electrodeless mercury-discharge lamp, Quarterly Progress Report No. 55, Research Laboratory of Electronics, M.I.T., October 15, 1959, p. 63.

#### E. ANODE DESIGN FOR MERCURY VAPOR DISCHARGE TUBE

The presence of relaxation oscillations at the anode of electric discharge tubes has proved troublesome in our experiments. A brief program has been started for the purpose of discovering anode structures free from oscillations.

These oscillations occur when electrons accelerated in a strong, positive-anode fall region ionize atoms. The positive ions then reduce the space charge, thereby stopping the ionization. When the space charge builds up again, ionization can take place, and the cycle is complete.

The strong anode fall occurs when the discharge is drawn to high-field regions such as anodes of small area or with sharp edges. In these regions the electron current density is much higher than it is in the plasma body, and a space charge arises. The necessary conditions for oscillations can be eliminated by neutralizing the space charge, or by preventing the discharge from being drawn to high-field regions.

The first scheme is due to Pupp.<sup>1</sup> The space charge is neutralized by running a discharge between an auxiliary cathode near the anode and the anode. The second method prevents the discharge from striking sharp-edged sections of the anode. This

## (V. NUCLEAR MAGNETIC RESONANCE)

can be accomplished by putting negative voltages on guard rings near the edges, or by using anodes with no sharp edges, or inhibiting the discharge near sharp-edged regions with magnetic fields. Of these, all except using an anode with no sharp edges have been tried, and all prevent oscillations. Our experiments are summarized below.

Several onode structures, described below, were installed in ordinary fluorescent tubes containing mercury vapor and argon at a pressure of 2 mm Hg. The current was varied between 0.5 and 2.0 amps. The phosphor of the tube acts as a getter. These tubes were provided by the Sylvania Electric Company.

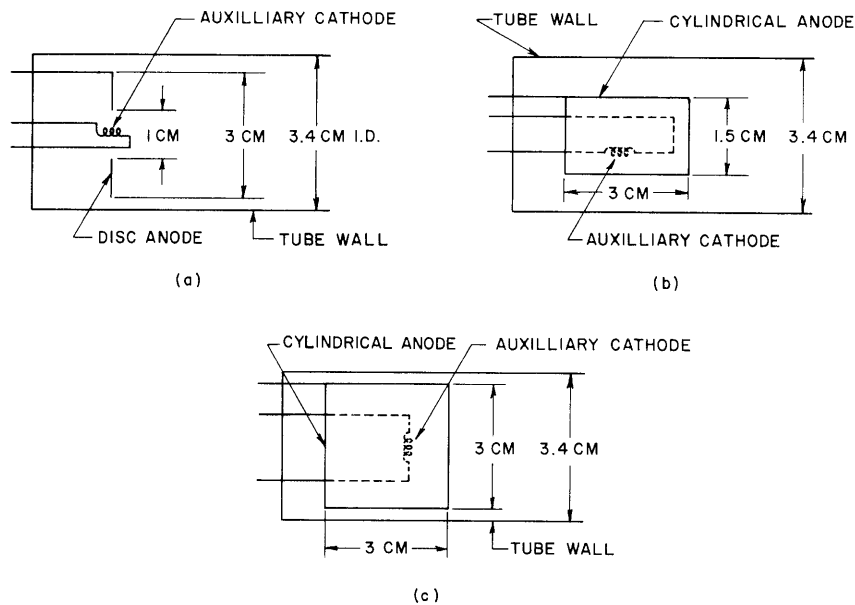


Fig. V-6. Anode structures with auxiliary cathodes.

Three configurations of the auxiliary cathode type were built. These are shown in Fig. V-6. In Fig. V-6a oscillations are present, and the discharge glow is visible in front and back of the disc until the auxiliary discharge of approximately 1 amp is turned on. After the auxiliary discharge is started the glow is confined to the front of the disc, and oscillations stop. In Fig. V-6b the glow is visible outside the cylinder, and oscillations are present without the auxiliary discharge. The oscillations vanish when the auxiliary discharge is lighted, and the glow appears to funnel into the end of the cylinder. Similar behavior is characteristic of Fig. V-6c, except that the discharge occasionally goes into the interior without the auxiliary discharge.

The configurations without auxiliary cathodes are shown in Fig. V-7. Shape V-7a oscillates, and the glow is seen around the outside when only one cylinder is used as an anode. When both are used in parallel the glow is confined to the interior and oscillations stop. In Fig. V-7b there is no glow outside, and no oscillations when the

(V. NUCLEAR MAGNETIC RESONANCE)

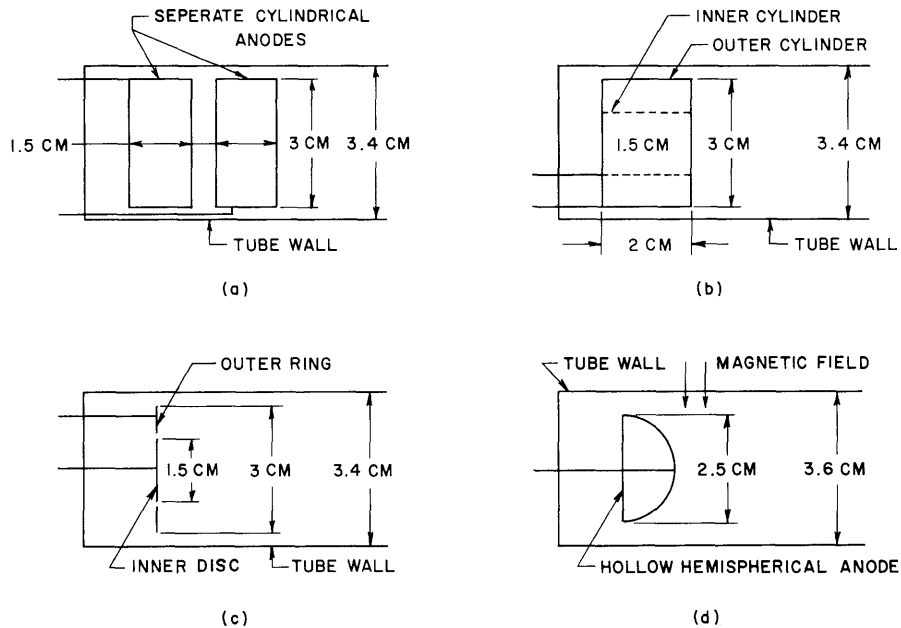


Fig. V-7. Anode structures without auxiliary cathodes.

inner cylinder is used as the anode, and the outer cylinder floats at a negative potential relative to the anode. If the two cylinders are at the same potential, or if the outer cylinder is used as the anode, oscillations occur. Similarly, in Fig. V-7c when the disc alone is the anode no oscillations occur, but when both the disc and the ring are used they are present. In Fig. V-7d the discharge ordinarily goes to the sharp edges at the back of the hemispherical anode and oscillations occur. This may be prevented by applying a transverse magnetic field that confines electron collection to the front of the electrode.

In the auxiliary cathode configurations space charge is neutralized by the auxiliary discharge, and the electrons pass easily to the anode. In the first two of the second series of anodes the electrons are deflected to the interior of the cylindrical anodes by the negative floating potential of the nearby walls or floating electrodes. Once inside, they can be collected in the low-field region of the interior, if the area is large enough. In the third series they are deflected to the plane surface of the center disc by the floating guard ring. In the fourth series the magnetic field prevents them from diffusing back to the sharp-edged section of the hemisphere.

T. Fohl, J. F. Waymouth

References

1. W. Pupp, Phys. Z. 33, 844 (1932); 34, 756 (1933).

